The 2010 IEEE/RSJ International Conference on
Intelligent Robots and Systems
October 18-22, 2010, Taipei, Taiwan

Energetics of Flapping-Wing Robotic Insects: Towards Autonomous Hovering Flight

Michael Karpelson, *Student Member, IEEE,* John P. Whitney, Gu-Yeon Wei, *Member, IEEE,*
Robert J. Wood, *Member, IEEE*

***Abstract*— Flapping-wing mechanisms inspired by biological insects have the potential to enable a new class of small, highly maneuverable aerial robots with hovering capabilities. In order for such devices to operate without an external power source, it is necessary to address a complex system design challenge: the integration of all of the required components on board the robot. This paper discusses the flight energetics of flapping-wing robotic insects with the goal of selecting design parameters that enable power autonomy and maximize flight time. The subsystems of the robot are analyzed both from a broad perspective and using a detailed set of models for a piezoelectrically driven two-wing design. The models are used to perform a system-level optimization for the maximum flight time permitted by current technology, compare the resulting robot configurations to biological insects across several key metrics, and discuss the effect of performance gains in various subsystems of the robot.**

***Index Terms*— Aerial robotics, biologically inspired robotics, flight energetics, MAV, microrobotics.**

I. Introduction

Flapping-wing robotic insects are a class of micro air vehicles (MAVs) that take design cues from their biological counterparts to achieve a small size, high maneuverability, and hovering ability. Several prototypes of flapping-wing robotic insects have shown promise, including the Micromechanical Flying Insect [1] and the Harvard Microrobotic Fly [2]. At present, robotic insects capable of hovering flight have not yet taken to the air without external power.

Significant progress has been made with regard to designing and optimizing the individual subsystems of flapping-wing robotic insects, including aerodynamic components [3], actuation [4], and power electronics [5]. However, the stringent weight and power requirements of insect-scale flight make it difficult to achieve fully autonomous operation without a thorough understanding of the interactions and tradeoffs between the various components, to a degree that cannot be captured by isolated models and optimizations.

The ultimate goals of studying MAV flight energetics are to achieve fully autonomous operation by placing all of the components required for flight on board the vehicle and to maximize the flight time of the vehicle by designing and integrating these components in an optimal manner. Continuing advances in the design and characterization of the various MAV subsystems have paved the way for the next important step towards these goals: an integrated, system-level model of a flapping-wing MAV. Such a model can focus the design effort from a system-level perspective and provide the ability to:

1) Analyze design tradeoffs and identify promising regions of the design space.
2) Enable system-level optimizations for various performance metrics.
3) Facilitate comparison to biological insects and other aerial platforms.
4) Identify the subsystems that have the greatest effect on a given performance metric.

This paper discusses general concepts, applicable to a broad range of MAVs, and presents a detailed model of a flapping-wing MAV based on the Harvard Microrobotic Fly. Section II presents a generalized formulation of MAV subsystems, design parameters, and figures of merit. Section III applies this generalized formulation to a specific design through a set of models and approximations that describe each MAV subsystem, including aerodynamic and mechanical components, actuation, power and control electronics, and the energy source. Section IV describes the results of system-level analyses performed using this modeling framework; these include maximizing flight time by selecting optimal points in the mass/flapping frequency design space, comparing the resulting configurations to biological insects in terms of mass, flapping frequency, wing area, and input power, and discussing how prospective improvements in various model parameters affect flight time.

II. Generalized Formulation for MAVs

To approach MAV design and optimization from a system-level perspective, it is useful to establish a generalized formulation, applicable to many different devices, that describes the components of a MAV. There are three primary subsystems involved in flight energetics: the aerodynamic components (wings), the power actuators, and the energy source. These subsystems are linked by two transduction mechanisms: the mechanical transmission, which serves as the interface between the actuator and the aerodynamic components, and the power electronics, which serve as the interface between the energy source and the actuator. The remaining subsystems may include: structural, control electronics, sensing, communications, and energy harvesting components.

In order to simplify the formulation and emphasize the focus on flight energetics, all MAV subsystems except for the aerodynamic components, the power actuators, and the energy source are classified as payload. Payload is divided into two categories: static payload, which has a fixed mass,

The authors are with the School of Engineering and Applied Sciences, Harvard University, Cambridge, MA 02138, USA (contact e-mail: michaelk@seas.harvard.edu)

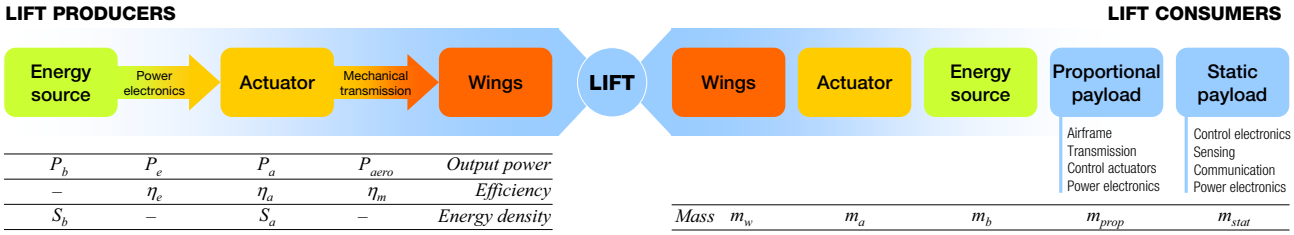

Fig. 1. Lift-generating and lift-consuming components of a generic MAV, and parameters related to each component.

and proportional payload, where the mass scales as a percentage of the total mass of the MAV. Based on previous design and fabrication experience, this is sufficient to capture most of the relevant scaling trends. Fig. 1 shows a diagrammatic representation of the lift-generating and lift-consuming subsystems of a generic MAV, as well as a list of parameters pertaining to each subsystem.

To enable autonomous flight, the sum of the masses of lift-consuming components (m_w, m_a, m_b, m_{prop}, and m_{stat}) must be less than or equal to the total generated lift. Moreover, when the parameters listed in Fig. 1 are known, it is possible to estimate the flight time of the robot using:

$$t_f = \frac{E_b \eta_e \eta_a \eta_m}{P_{aero}} \tag{1}$$

where E_b is the energy capacity of the battery and the other parameters are as defined in Fig. 1.

A. Mass and efficiency tradeoffs

The large design space of many MAV subsystems presents an opportunity to introduce efficiency improvements at the cost of increased mass, or, conversely, reduce the mass of a component at the cost of efficiency. It is helpful to evaluate the benefit of such design choices by considering their effect on flight time. For example, assuming the MAV mass is kept constant, a more efficient component may actually reduce flight time if the associated mass increase reduces the size of the energy source to a sufficient degree. Hence, if the goal is to prevent the reduction of flight time, a change Δm in the mass of a component that is accompanied by a corresponding change $\Delta\eta$ in the total efficiency (defined as the product of η_e, η_a, and η_m) must satisfy the condition that the energy lost from shrinking the energy source by Δm is balanced by the energy gained from the efficiency improvement $\Delta\eta$.

In addition, the flight time will depend not only on the quantity of energy stored in the battery, but also on the battery discharge rate, or C-rate, which is defined as the discharge current expressed in multiples of the rated capacity in Ampere-hours. The effective battery capacity will generally decrease from the rated value as the C-rate increases; however, because the relationship between the C-rate and the effective capacity is highly dependent on the specific battery, it is not possible to estimate what increase in C-rate can be tolerated without decreasing flight time. It is possible, however, to specify that a change Δm in mass that is accompanied by a corresponding change $\Delta\eta$ in efficiency must not increase the C-rate, by satisfying the following inequality:

$$(m_b + \Delta m)(\eta + \Delta\eta) \geq m_b \eta \tag{2}$$

where m_b is the mass of the energy source and η is the total efficiency. Satisfying the inequality therefore ensures that the design modification does not affect flight time negatively.

B. Mass and power budget tradeoffs

The majority of the power budget in a hover-capable MAV is allocated to subsystems which enable flight – a fact mirrored in biological insects, where flight metabolic rates exceed resting metabolic rates by a factor of 50-100 [6]. However, due to the limited energy storage on board the MAV, mass and power budgeting for components that are not directly involved in lift generation, such as sensors and control electronics, can also become important. At design time, such mass and power budgets are interdependent quantities: as the mass of a component is reduced, its power budget can be increased without affecting operating time because the mass savings can be used to increase the size of the energy source.

To give maximum leeway to the designers of such components, it is helpful to present the mass and power budget as related metrics. The following expression gives Δp, the power budget change based on a change Δm in the mass budget that can be tolerated without affecting the C-rate, and therefore the flight time:

$$\frac{P_b + \Delta p}{E_b + S_b \Delta m} \leq \frac{P_b}{E_b} \tag{3}$$

where E_b and P_b are the battery energy capacity and power draw, prior to any modifications, and other quantities are as defined previously.

III. System-Level Model of a Flapping-Wing Robotic Insect

The models used in this analysis are based on the design and fabrication paradigms of the Harvard Microrobotic Fly (Fig. 2) – a flapping-wing robotic insect with two wings powered by a piezoelectric bimorph actuator. This paper adopts a top-down approach that begins with the mass and flapping frequency of a hypothetical vehicle and uses these values to determine successively the power P_{aero}, the requirements for the mechanical components, the design of the actuator and power electronics, the size of the energy

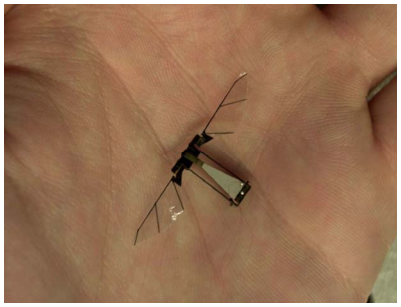

Fig. 2. Harvard Microrobotic Fly.

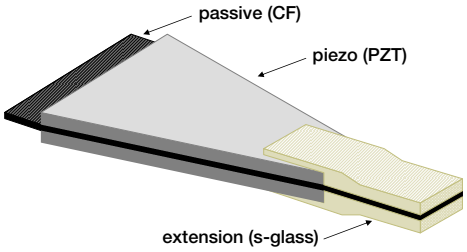

Fig. 4. Piezoelectric bimorph structure.

source, and the available payload. This makes it possible to estimate the flight time of the robot, per Eq. 1. The key aspects of the components that comprise the system-level model are described below.

A. Aerodynamic components

In order to make the aerodynamic design tractable for the purposes of this analysis, a simple blade-element aerodynamic model is used to determine the mechanical and power requirements for hovering. The blade element approach is very similar to analyses in [1], [7], where additional details can be found. The wing is divided into chord-wise strips, and the force coefficients, which are a function of angle of attack, are provided by previous experiments with dynamically scaled wing models [7].

Several approximations have to be made in order to reduce the very large design space of a flapping vehicle's wings to manageable proportions. This model assumes two wings with an aspect ratio of 4 (wing length over mean chord) flapping in the horizontal plane with symmetric and sinusoidal flapping and rotation kinematics. The total flapping angle is fixed at 120 degrees, and the mid-flap angle of attack is 45 degrees, which is in line with previous experimental results [2]. Futhermore, the wing center of area is taken at half-span, with the second moment of area derived from Ellington's empirical relationship [8], which corresponds to previous assumptions in similar models [9].

The aerodynamic model is used to determine input power and wing characteristics for MAVs of a given mass and flapping frequency. For any point in the mass-frequency space, the wing length is iterated over (keeping the aspect ratio constant) until the lift generated equals the desired mass of the MAV. The vehicle is assumed to be hovering in place, so the input power to the wings is obtained from the profile power (viscous losses) calculated from the blade-element model. Any inertial power is assumed to be fully recovered from the elastic storage within the actuator and transmission.

This method produces MAV configurations that follow a set of well-defined power laws. The input power to the wings follows the relationship:

$$P_{aero} \propto f^{0.5} L^{1.25} \tag{4}$$

while the wing area follows the relationship:

$$A_{wing} \propto f^{-1} L^{0.5} \tag{5}$$

where f is the flapping frequency and L is the lift generated. Fig. 3 shows the values of input power and wing area obtained using the blade-element model as well as a surface fitted to the data using the above relationships for a range of lift values and flapping frequencies.

B. Mechanical components

The mechanical components of the MAV are fabricated using the Smart Composite Microstructures (SCM) process [10], which enables the integration of rigid structural links made of carbon fiber with low-loss polymer flexures that are over 90% efficient [11] (flexures are used instead of friction-based transmission mechanisms, such as gears and sliders, due to unfavorable scaling of surface effects as device size is reduced). SCM is used to produce the airfoils, airframe, wing hinges, and the mechanical transmission that couples the actuator to the wings. The input power to the wings, derived from the aerodynamic model, is used together with the wing kinematics to design wing hinges and a mechanical transmission that can generate the required wing motion. The power and kinematics data, along with the transmission ratio, can then be used to identify the force and displacement requirements for the actuator.

C. Actuation

Piezoelectric actuators are attractive in microrobotic applications due to their compact size and high power density. At the scales of flapping-wing robotic insects, they are expected to outperform both DC motors and a number of other microactuation technologies [11]. This analysis assumes composite piezoelectric bimorph actuators optimized for energy density, described in detail in [4] and used in the Harvard Microrobotic Fly.

Fig. 4 shows the structure of the actuator. The actuator is compatible with the SCM process and fabricated using laser micromachining. This analysis uses previously developed models for the free-end deflection, blocked force, and operating frequency of piezoelectric bimorph actuators as a function of actuator geometry, material properties, and applied excitation; details can be found in [4] and [12]. MATLAB scripts are used to automatically produce an actuator geometry that satisfies the force and displacement requirements dictated by the wing input power and transmission design.

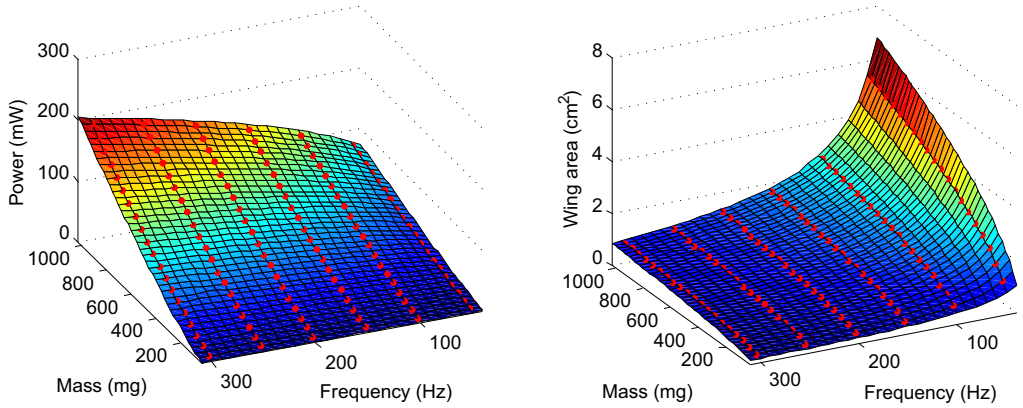

Fig. 3. Results for input power and wing area obtained using the blade element model (points) and a surface fitted to the data using equations 5 and 6.

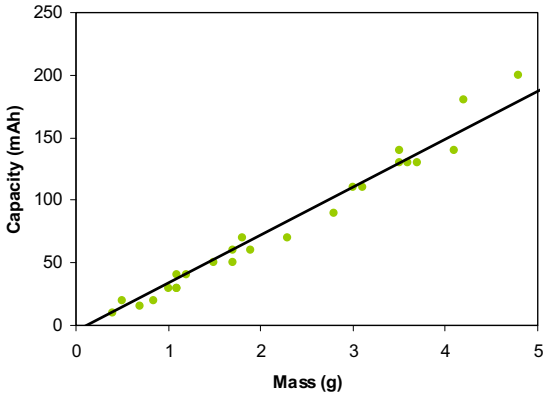

Fig. 5. Mass and capacity trends of Fullriver lithium polymer batteries.

The actuators are driven at high fields in order to maximize energy density, necessitating drive voltages of 200-300V. The loss mechanisms include dielectric losses, hysteresis losses, and the coupling of energy into mechanical resonant modes that do not contribute to wing flapping. For a given actuator geometry and driving conditions, these losses can be modeled using an equivalent electrical circuit [5].

D. Energy source

Promising energy sources for robotic insects include conventional batteries, fuel cells, ultracapacitors, and solar cells. At present, however, lithium polymer batteries are the only developed, commercially available technology that can satisfy the requirements of insect-sized MAVs. Fig. 5 shows the capacity of several Fullriver batteries. This analysis assumes a single-cell lithium polymer battery with a nominal voltage of 3.7V and an arbitrary capacity that scales according to the trend of Fig. 5.

The energy source model is complicated by the fact that the capacity of lithium polymer batteries decreases at high discharge rates. The properties of the capacity derating depend heavily on the battery design and manufacturing parameters. As a result, it is difficult to estimate battery performance without a specific battery in mind; at the same time, it is important to consider derating because the high power requirements of hovering MAVs inevitably translate to high battery discharge rates. This analysis adopts a linear derating model, where the battery maintains the rated capacity at a discharge rate of 1C and the capacity derates linearly with increasing C-rate until it is reduced to zero at 30C. These assumptions are also based on Fullriver lithium polymer batteries, which advertise continuous discharge rates of 10-20C and burst discharge rates (under 5 seconds) of 20-40C. In practice, however, the derating relationship may be nonlinear.

Note that, although the current analysis assumes a particular battery technology, the modularity of the system-level model means that it can easily be adapted to new energy sources as they continue to emerge. Promising technologies include micro solid oxide fuel cells [13], lithium batteries with silicon nanowire anodes [14], and lithium air batteries [15].

E. Power and control electronics

The power electronics must be capable of converting the low input voltage from the energy source into a time-varying, high-voltage drive signal capable of powering a piezoelectric actuator. Such a drive signal must be unipolar (i.e. only positive or only negative) in order to achieve high deflection in the actuator without depolarizing the piezoelectric layers [4]. Moreover, because only a fraction of the input electrical energy is converted by the actuator into mechanical output, it is highly desirable for the drive electronics to be capable of recovering unused energy from the actuator for use in subsequent actuation cycles.

The power electronics functionality is realized using high-voltage switching drive stages which can both generate an arbitrary drive signal and recover energy from the actuator. Fig. 6 shows two such circuit topologies; additional details and experimental results using discrete components can be found in [5]. The goal of the power electronics design effort is a maximally integrated system which includes custom

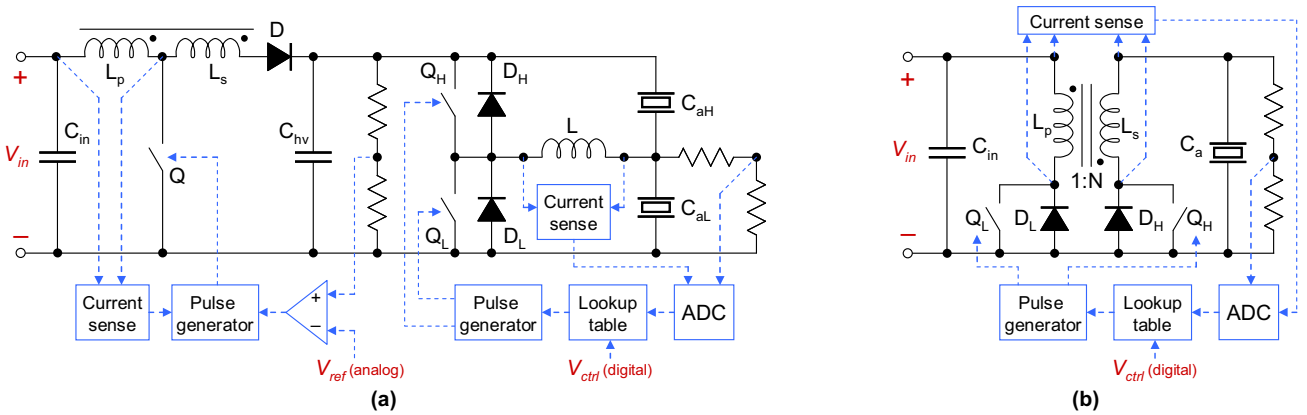

Fig. 6. Lightweight circuit topologies suitable for driving piezoelectric actuators. A tapped inductor boost converter combined with a switching amplifier drive stage (a) converts the input voltage to a constant high-voltage bias which is then used to produce a drive signal across piezoelectric layers C_{aH} and C_{aL}, representing a bimorph actuator. The bidirectional flyback converter (b) simultaneously steps up the voltage and generates a drive signal across piezoelectric layer C_a, representing a unimorph actuator or a single layer of a bimorph. In both cases, an A/D converter monitors the actuator voltage, which is then adjusted by modulating the semiconductor switches.

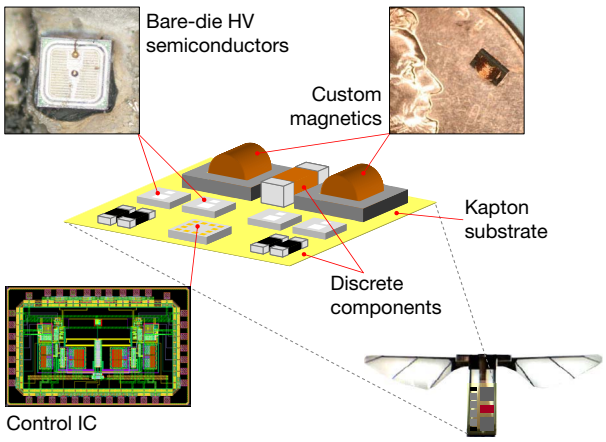

Fig. 7. Target implementation of a high-voltage power electronics package.

magnetic components, bare-die power semiconductors, discrete components, and a custom integrated control circuit (Fig. 7).

The mass of the power electronics is determined using commercial device data, experimental results from power electronics packages assembled using both discrete and bare die components, and mass calculations for custom-built magnetic components. Efficiency is estimated using a series of MATLAB scripts that model various loss mechanisms, which include conduction, switching, and magnetic losses. Although the details of the sensing and control architecture have not been finalized, previous work on lightweight flight control sensors [16] and low-power microcontrollers [17] is used to estimate the payload requirements of a hypothetical MAV "brain."

TABLE I
OPTIMIZATION ASSUMPTIONS

Parameter	Value	Source
Battery energy density	450 kJ/kg	Commercial battery data
Actuator energy density	3 J/kg	Actuator models
Power electronics efficiency	70 %	Efficiency models and experimental results
Static payload	20 mg	Experimental results and commercial device data
Proportional payload	25 %	Experimental results commercial device data

IV. Design Space Analysis

The modeling framework described in the previous section allows a systematic exploration of the design space with the goal of maximizing the operating time of a hypothetical flapping-wing robotic insect. Of particular interest is the selection of vehicle mass and flapping frequency, as these are fundamental design choices that influence most of the robot's subsystems and cannot be changed without redesigning a number of key components. It is therefore highly desirable to examine the mass/flapping frequency space in advance in order to identify design regions that allow for maximum flight time.

The optimization procedure necessitates certain assumptions about the performance of the various MAV components. Table I lists relevant model parameters, the chosen values, and the sources used to obtain these values. The values are based on the current state of the art in the corresponding subsystems and, in some cases, incorporate expected improvements over current experimental results.

A. Optimization results and biological trends

Figures 8, 9, 10, and 11 show the optimization results in the context of several metrics: vehicle mass, flapping

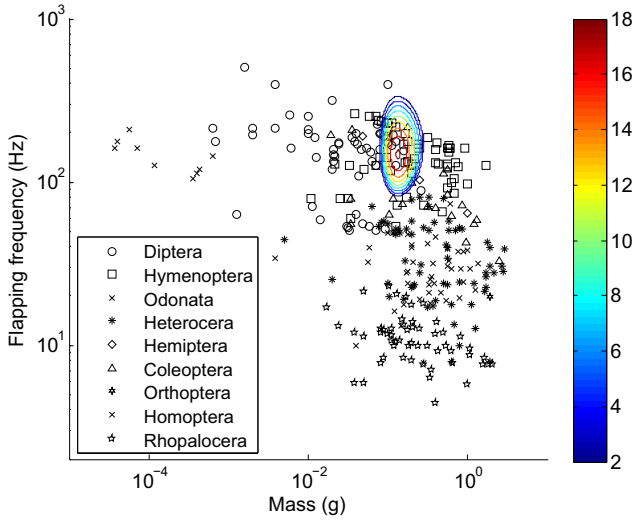

Fig. 8. Flight time optimization results in the mass vs. flapping frequency space, overlaid on biological insect data (Dudley data set). Contour color bar indicates flight time (s).

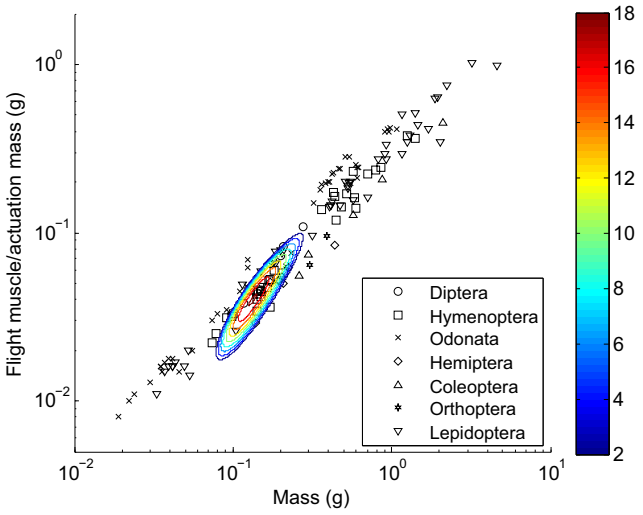

Fig. 10. Flight time optimization results in the vehicle mass vs. actuation (flight muscle) mass space, overlaid on biological insect data (Marden data set). Contour color bar indicates flight time (s).

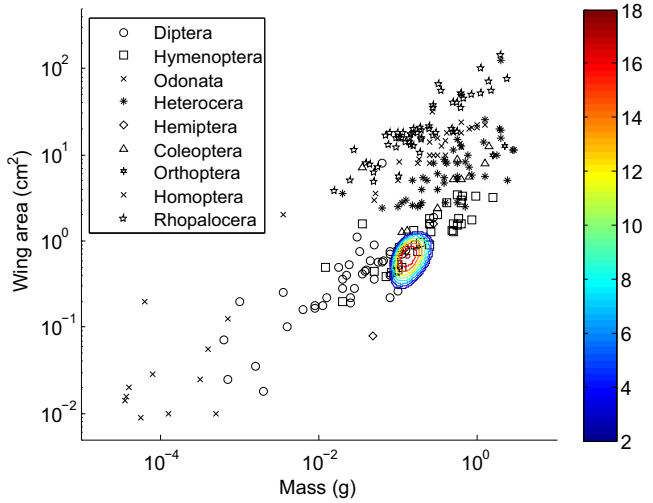

Fig. 9. Flight time optimization results in the mass vs. wing area space, overlaid on biological insect data (Dudley data set). Contour color bar indicates flight time (s).

frequency, wing area, actuation (or flight muscle) mass, and input power. Fig. 12 shows the mass allocation to the various robot subsystems in the optimal configuration, a 135mg device that flaps its wings at 146Hz. Wherever possible, the optimization results are compared with biological insect data. There are no biological data sets with data across all of the metrics of interest; thus, flapping frequency and wing area data are obtained from Dudley [18], flight muscle mass is obtained from Marden [19], and input power (estimated using flight metabolic rate) is obtained from Niven and Scharlemann [20]. As a result, the biological data in the different figures is *not* always taken from the same dataset. Rather, the goal is to compare optimization results to the largest amount of biological data for each metric.

Biological insects represent an important baseline for bio-inspired robotic insects. While a robotic insect configuration that falls within the trends defined by biological insects does not guarantee a successful design, a robotic insect with parameters that differ greatly from biological trends may be cause for concern. As seen in Figures 8, 9, and 10, the optimization produces robotic insect configurations that follow biological trends with regard to overall mass, wing flapping frequency, wing area, and actuator (flight muscle) mass. The optimal configurations most closely resemble biological insects of the orders Diptera (flies) and Hymenoptera (bees). Fig. 11 compares the electrical power drawn from the battery of robotic insects to the metabolic power of biological insects (obtained using flight metabolic rates and using a standard conversion factor of 20J of chemical energy per ml O_2 consumed [6]); although robotic insects consume more power, the difference is less than an order of magnitude.

Despite many similarities, robotic insects are outperformed by their biological counterparts in a number of key areas, including flight time. The optimization results show that, assuming the current state of the art as described in Table I, robotic insects will only be able to remain aloft for about 18 seconds. Although it is difficult to quantify maximum operating time in biological insects, it is measured in minutes or hours; insects can store more energy and convert it into mechanical output more efficiently. Biological insects also exhibit better aerodynamic performance, which allows them to lift more than their body weight (the robotic configurations in this analysis were designed for a thrust-to-weight ratio of 1, in order to maximize flight time). Increasing the flight time and aerodynamic performance of robotic insects will require improvements in the performance of lift-generating MAV subsystems.

B. *Effect of performance enhancements*

An increase in flight time will require improvement in one or more of the model parameters listed in Table I.

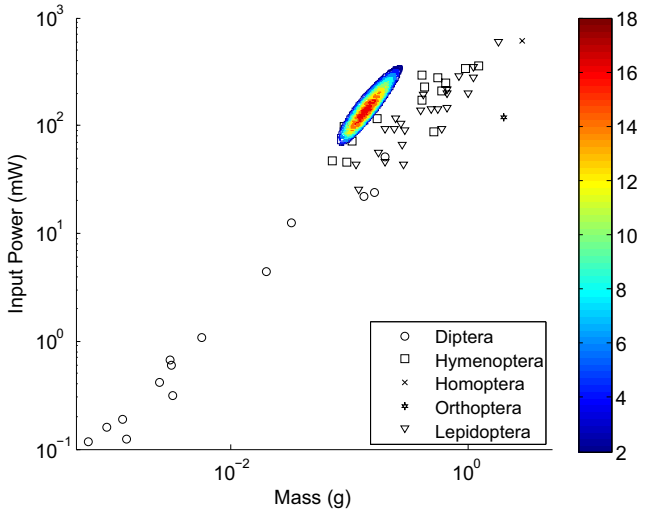

Fig. 11. Flight time optimization results in the mass vs. input power space, overlaid on biological insect data (Niven and Scharlemann data set). Input power refers to electrical power for robotic devices and metabolic power for biological insects. Contour color bar indicates flight time (s).

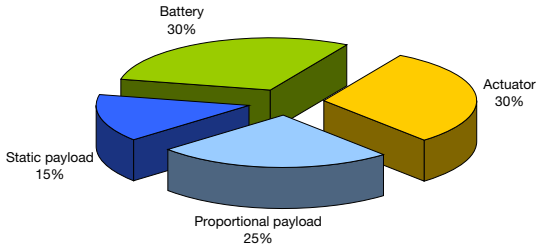

Fig. 12. Mass budget breakdown for the optimal robotic insect configuration: a 135mg vehicle with a wing flapping frequency of 146Hz. Wings account for less than 1% of the mass, and are not shown.

Here, improvement is defined as a reduction in mass or an increase in efficiency or energy density. Furthermore, since a vehicle hovering in place does not perform any work, an improvement in aerodynamic efficiency is defined as a reduction in the input power to the wings per unit lift. A system-level model can be useful in determining the extent to which the various model parameters affect the length of time an MAV may remain aloft before recharging. Together with information on the feasibility of potential improvements and the limits to these improvements, it is possible to identify the most promising areas of research with regard to increasing MAV flight time.

Table II lists, in relative terms, the effect of the parameters of Table I on MAV flight time, the capacity for improvement (i.e. the degree of improvement allowed by the theoretical bounds of the associated technology), and the feasibility of achieving this improvement based on technological limitations and previous fabrication experience. Also listed are potential methods to achieve this improvement and some of the known quantitative bounds on these methods.

As may be expected, the performance of aerodynamic components has a significant effect on flight time: if less power can be used to generate a given amount of lift, this translates to relaxed requirements on the actuator and the power electronics, a consequent reduction in the mass of these subsystems, and increased room for the battery. Ongoing research efforts are directed at optimizing wing motion, shape, and mechanical properties using biological insect data as a guide. Less intuitive is the idea that power electronics efficiency has a very significant effect on flight time. This can be explained by the low electromechanical coupling coefficient of the piezoelectric actuators considered in this analysis: during any given wing stroke, the power electronics must transfer much more electrical energy to and from the actuator than is converted into mechanical output. An increase in power electronics efficiency therefore translates to significant energy savings and a corresponding increase in flight time.

Battery energy density has a less pronounced effect on flight time, but there is significant potential for improvement as new battery technologies continue to emerge in the coming years – many of these have the potential to exceed the energy density of today's lithium polymer batteries by a factor of 10 or more. Although previous work on piezoelectric actuators has produced designs optimized for energy density under d_{31} actuation (deflection parallel to electric field), it may be possible to extract additional performance gains by improving the actuator strain limit to allow operation under the maximum possible electric field (producing maximum deflection), or by redesigning the actuator to use d_{33} actuation (deflection orthogonal to electric field), which allows better electromechanical coupling. Actuator design is also relevant to power electronics; using thinner piezoelectric layers enables reduced operating voltages, which can boost the efficiency of power circuits.

Althought model parameters associated with lift generation have a more pronounced effect on flight time and generally exhibit a greater capacity for improvement, lowering the mass of the payload is also an important consideration. Some improvement in the payload metrics is expected to arise naturally during final system integration, which will require lightweight, efficient methods for packaging the components and incorporating them into the structure of the MAV.

V. Summary

This paper discusses system-level modeling of flapping-wing robotic insects with a focus on flight energetics, power autonomy, and maximizing flight time. The analysis supports the feasibility of designing piezoelectrically driven robotic insects, modeled after the Harvard Microrobotic Fly, that can take off without external power. Such robotic insect designs follow biological trends and exhibit particular similarities to biological insects of the orders Diptera and Hymenoptera. While current technology is expected to yield devices that can remain aloft for less than a minute, incremental advances in the lift-generating subsystems of the robot are expected to increase the maximum flight time before recharging.

TABLE II

OPPORTUNITIES FOR PERFORMANCE ENHANCEMENT

Parameter	Effect on flight time[a]	Capacity for improvement[b]	Feasibility of improvement[c]	Potential methods	Limitations
Aerodynamic efficiency[d]	●●●●	●●●	●●●	Wing shape and stiffness profile optimization, wing kinematics optimization, stroke plane deviation [21].	Biological data can help establish the bounds on aerodynamic efficiency. Some hovering insects have estimated power densities as low as 16W/kg [22].
Battery energy density	●●	●●●●	●●●●	Promising technologies include Si nanowire batteries, Li-air batteries, micro fuel cells.	Theoretical energy densities: >3.6MJ/kg for fuel cells [13], 5.9MJ/kg for nanowire batteries [14], 18.7MJ/kg for Li-air [15].
Actuator energy density	●●	●●●	●●	Strain limit improvements, d_{33} actuation (deflection orthogonal to electric field).	Maximum strain energy density for bulk free plate (PZT-5H) is 4.0J/kg for d_{31} actuation [4].
Power electronics efficiency	●●●●	●●	●●	Circuit component optimization, actuation voltage reduction through thinner piezo materials.	Efficiency models project about 75-80% peak theoretical efficiency at current actuation voltages.
Static payload	●	●	●	Airframe structural optimization, integration of components into airframe, novel packaging for semiconductors and sensors.	Previous fabrication experience suggests a lower bound of about 20% on the payload mass fraction.
Proportional payload	●●	●	●●		

[a] Obtained from parametric study of system-level MAV model.
[b] Based on simulations and theoretical technological limits.
[c] Based on known technological limitations and fabrication experience.
[d] An improvement in aerodynamic efficiency is defined as the reduction of input aerodynamic power per unit lift.

Future work will include the experimental validation of the system-level model by fabricating robotic insect prototypes within the favorable mass and flapping frequency ranges identified during optimization, and evaluating their performance.

VI. ACKNOWLEDGEMENTS

The authors gratefully acknowledge support from the National Science Foundation (award number CCF-0926148). Any opinions, findings, conclusions, or recommendations expressed in this material are those of the authors and do not necessarily reflect those of the National Science Foundation. The authors also acknowledge support of the Wyss Institute for Biologically Inspired Engineering.

REFERENCES

[1] S. Avadhanula, "Design, fabrication, and control of the micromechanical flying insect," Ph.D. dissertation, U. C. Berkeley, 2006.
[2] R. J. Wood, "Liftoff of a 60mg flapping-wing MAV," in *IEEE/RSJ Int. Conf. on Intelligent Robots and Systems*, 2007, pp. 1889–1894.
[3] J. P. Whitney and R. J. Wood, "Aeromechanics of passive rotation in flapping flight," *Journal of Fluid Mechanics*, in press, 2010.
[4] R. J. Wood, E. Steltz, and R. S. Fearing, "Optimal energy density piezoelectric bending actuators," *Sensors & Actuators: A. Physical*, vol. 119, no. 2, pp. 476–488, 2005.
[5] M. Karpelson, G.-Y. Wei, and R. J. Wood, "Milligram-scale high-voltage power electronics for piezoelectric microrobots," in *IEEE Int. Conf. on Robotics and Automation*, 2009, pp. 883–890.
[6] C. P. Ellington, "Power and efficiency of insect flight muscle," *J. of Experimental Biology*, vol. 115, pp. 293–304, 1985.
[7] S. P. Sane and M. H. Dickinson, "The aerodynamic effects of wing rotation and a revised quasi-steady model of flapping flight," *J. of Experimental Biology*, vol. 205, no. 8, pp. 1087–1096, April 2002.
[8] C. P. Ellington, "The aerodynamics of hovering insect flight II: Morphological parameters," *Phil. Trans. R. Soc. B*, vol. 305, no. 1122, pp. 17–40, 1984.
[9] C. P. Ellington, "The novel aerodynamics of insect flight: Applications to micro-air vehicles," *J. of Experimental Biology*, vol. 202, no. 23, pp. 3439–3448, December 1999.
[10] R. J. Wood, S. Avadhanula, R. Sahai, and F. R. S., "Microrobot design using fiber reinforced composites," *J. of Mechanical Design*, vol. 130, no. 5, 2008.
[11] E. Steltz, M. Seeman, S. Avadhanula, and R. S. Fearing, "Power electronics design choice for piezoelectric microrobots," in *IEEE/RSJ Int. Conf. on Intelligent Robots and Systems*, 2006, pp. 1322–1328.
[12] Q. M. Wang and L. E. Cross, "Performance analysis of piezoelectric cantilever bending actuators," *Ferroelectrics*, vol. 215, no. 1-4, pp. 187–213, 1998.
[13] A. Evans, A. Bieberle-Htter, J. L. M. Rupp, and L. J. Gauckler, "Review on microfabricated micro-solid oxide fuel cell membranes," *J. of Power Sources*, vol. 194, no. 1, pp. 119–129, 2009.
[14] K. C. Chan, *et al.*, "High performance lithium battery anodes using silicon nanowires," *Nature Nanotechnology*, vol. 3, pp. 31–35, 2008.
[15] B. Kumar, *et al.*, "A solid-state, rechargeable, long cycle life lithium-air battery," *J. of the Electrochem. Soc.*, vol. 157, no. 1, pp. A50–A54, 2009.
[16] W. C. Wu, L. Schenato, R. J. Wood, and R. S. Fearing, "Biomimetic sensor suite for flight control of a micromechanical flying insect: design and experimental results," in *IEEE Int. Conf. on Robotics and Automation*, vol. 1, 2003, pp. 1146–1151.
[17] B. A. Warneke and K. S. J. Pister, "An ultra-low energy microcontroller for smart dust wireless sensor networks," in *IEEE Int. Solid-State Circuits Conf. 2004*, vol. 1, 2004, pp. 316–317.
[18] R. Dudley, *The Biomechanics of Insect Flight: Form, Function and Evolution*. Princeton University Press, 1999.
[19] J. H. Marden, "Maximum lift production during takeoff in flying animals," *J. of Experimental Biology*, vol. 130, no. 1, pp. 235–258, 1987.
[20] J. E. Niven and J. P. Scharlemann, "Do insect metabolic rates at rest and during flight scale with body mass?" *Biology Letters*, vol. 1, no. 3, pp. 346–349, 2005.
[21] B. M. Finio, J. P. Whitney, and R. J. Wood, "Stroke plane deviation for a microrobotic fly," in *IEEE/RSJ Int. Conf. on Intelligent Robots and Systems*, 2010.
[22] M. Sun, "High-lift generation and power requirements of insect flight," *Fluid Dynamics Research*, vol. 37, no. 1-2, pp. 21–39, 2005.